Research Square

Preprints are preliminary reports that have not undergone peer review.
They should not be considered conclusive, used to inform clinical practice,
or referenced by the media as validated information.

Graft Diameter Differentially Affects ACL Stress Across Flexion Angles: A Finite Element Analysis With Native Knee Control

Shaolong Du
First Affiliated Hospital of Guangdong Pharmaceutical University
XIshan Li
First Affiliated Hospital of Guangdong Pharmaceutical University
Qiang Lin
First Affiliated Hospital of Guangdong Pharmaceutical University
Xuehui Luo
man1028@126.com

First Affiliated Hospital of Guangdong Pharmaceutical University

Research Article

Keywords: anterior cruciate ligament reconstruction, graft diameter, finite element analysis, knee biomechanics, peak stress, native knee control

Posted Date: November 16th, 2026

DOI: https://doi.org/10.21203/rs.3.rs-11457178/v1

License: This work is licensed under a Creative Commons Attribution 4.0 International License.
Read Full License

Additional Declarations: No competing interests reported.

Graft Diameter Differentially Affects ACL Stress Across Flexion Angles: A Finite Element Analysis With Native Knee Control

Shaolong Du[1], Xishan Li[1], Qiang Lin[1], Xuehui Luo[1,*]

[1] Department of Orthopedics, The First Affiliated Hospital of Guangdong Pharmaceutical University, Guangzhou, Guangdong, China

*Corresponding author: Xuehui Luo, Department of Orthopedics, The First Affiliated Hospital of Guangdong Pharmaceutical University, Guangzhou, Guangdong, China. E-mail: man1028@126.com; Tel: +86-13674047120

Co-corresponding author: Qiang Lin, Department of Orthopedics, The First Affiliated Hospital of Guangdong Pharmaceutical University, Guangzhou, Guangdong, China. E-mail: qiang_linm@163.com; Tel: +86-13560393808

Abstract

Background. Graft diameter is a critical determinant of anterior cruciate ligament (ACL) reconstruction outcomes, but its biomechanical effect under physiological motion remains incompletely understood. This study quantified graft stress across three diameters against a native knee control.

Methods. A validated finite element knee model served as native control; reconstruction models with 7, 8, and 9 mm grafts shared identical anatomical parameters. Six flexion angles (0°–90°) and five loading conditions were applied (120 analyses: 30 native, 90 reconstructed). Peak von Mises stress of grafts and posterior cruciate ligament (PCL) was quantified.

Results. Mean ACL peak stress was 12.16 ± 4.94 MPa (7 mm), 14.31 ± 6.24 MPa (8 mm), and 17.00 ± 8.07 MPa (9 mm; diameter: $F = 17.92$, $P < 0.001$; flexion angle: $F = 55.73$, $P < 0.001$; interaction: $F = 2.74$, $P = 0.006$). The diameter effect peaked at 90° deep flexion, where 9 mm graft stress reached 30.47 MPa under external rotation, 42.5% above native. At 15° external rotation, grafts reached 7.4–9.3 times native stress (absolute increment, 12–16 MPa). The diameter effect size was greatest under external rotation ($\eta^2 = 0.126$). PCL stress increased mildly (approximately 1.30–1.37× native).

Conclusions. Larger graft diameters are associated with higher peak ACL stress, concentrated at two clinically relevant positions—90° deep flexion and 15° flexion with external rotation—while reconstructed grafts operated below native stress in 56% of rotation conditions. The 8 mm graft offered the most favorable loading trade-off. Peak-stress findings warrant average-stress validation.

Keywords: anterior cruciate ligament reconstruction; graft diameter; finite element analysis; knee biomechanics; peak stress; native knee control

Background

Anterior cruciate ligament (ACL) rupture is one of the most common sports-related knee injuries, with an estimated incidence of 30–78 per 100,000 person-years [7,19]. ACL reconstruction aims to restore knee stability and prevent secondary meniscal and cartilage damage, which are associated with early-onset osteoarthritis [1]. Graft diameter is widely regarded as a critical determinant of reconstruction success, with larger grafts traditionally assumed to provide superior structural stiffness and lower failure risk [9,15].

However, clinical outcomes with large-diameter grafts are inconsistent. Some patients develop early anterior knee pain, limited range of motion, and late laxity despite receiving large grafts [13,22]. This suggests that the relationship between graft diameter and clinical outcome is not simply linear. Previous finite element studies of the knee have largely focused on conditions such as cartilage degeneration and meniscal injury rather than comparing reconstructed knees with a native control baseline [5,14], making it difficult to determine whether reconstruction restores physiological ligament stress levels.

This study established a native knee control model and systematically compared three graft diameters (7, 8, 9 mm) across six flexion angles and five loading conditions. The primary objective was to quantify the deviation of reconstructed ACL stress from physiological levels and identify high-risk positions for each graft size. It was hypothesized that larger graft diameters would be associated with higher peak intra-graft stress, with the magnitude of the diameter effect varying across flexion positions.

Methods

Model Construction

A complete native knee model was reconstructed from CT and MRI data of a healthy adult male volunteer using Mimics 21.0 (Materialise, Belgium), Geomagic Studio 2013 (3D Systems, USA), SolidWorks 2017 (Dassault Systèmes, France), and ANSYS 17.0 (ANSYS Inc., USA). The model included femur, tibia, fibula, patella, meniscus, articular cartilage, and cruciate ligaments. The native model mesh comprised approximately 270,000–400,000 elements across six flexion angles, with refined element sizes in ligament and cartilage regions. The assembled finite element model is shown in Figure 1.

[Figure 1 near here]

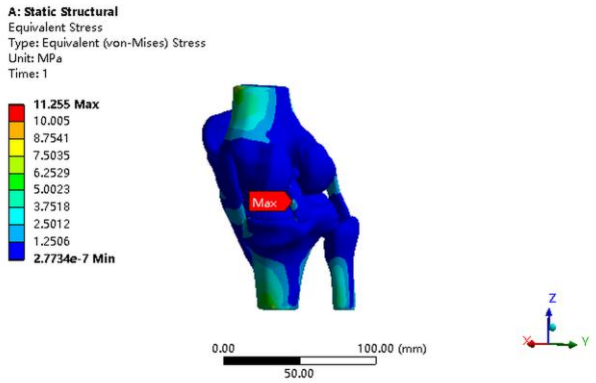


Figure 1. Three-dimensional finite element model of the knee joint, including bony structures, menisci, articular cartilage, and cruciate ligaments.

Material Properties

All tissues were modeled as homogeneous, isotropic, linearly elastic materials. Material parameters were derived from published knee biomechanical literature [2,8,16,17] (Table 1). Reconstructed grafts were assigned identical material properties to native ACL to isolate diameter as the sole independent variable.

Table 1. Material properties of knee joint structures

Tissue Structure	Elastic Modulus (MPa)	Poisson's Ratio
Patella and femur	1200	0.38
Tibia and fibula	6900	0.49
ACL graft (hamstring tendon)	116	0.30
Native ACL	116	0.30
PCL	87	0.30
Collateral ligaments	48	0.30
Articular cartilage	5	0.46
Medial and lateral menisci	5	0.46

Reconstruction and Loading Conditions

Three ACL reconstruction models with graft diameters of 7 mm, 8 mm, and 9 mm were established using standard anatomic single-bundle reconstruction. All tunnel positions, graft tension, and fixation methods remained identical. Six flexion angles (0°, 15°, 30°, 45°, 60°, 90°) and five loading conditions were simulated: 8 N·m internal rotation, 8 N·m external rotation, 20 N·m varus, 20 N·m valgus, and a 134 N posteriorly directed load applied to the femur (equivalent to anterior tibial translation) [3,12,18]. All loading conditions were superimposed on a 700 N axial compressive preload. These load levels correspond to the extreme external loads encountered during clinical examination maneuvers and vigorous sports—above the level of routine gait—allowing assessment of the upper-bound mechanical response of the graft; muscle forces further modulate joint contact and ligament loading [3]. The native knee model served as control. A total of 120 analyses were performed (30 native + 90 reconstructed).

Statistical Analysis

Descriptive statistics were reported as mean ± standard deviation (SD), median, and 95% confidence interval (CI). One-way analysis of variance (ANOVA) was used to compare ACL stress among the three graft diameters, with effect sizes reported as eta-squared (η^2) and Cohen's f. Post-hoc pairwise comparisons were performed using Bonferroni correction, with effect sizes reported as Cohen's d.

Two-way ANOVA was conducted to evaluate the main effects of graft diameter and flexion angle, as well as their interaction, on ACL stress. Multiple linear regression was performed to quantify the independent contribution of each predictor (diameter, angle, and loading condition, all entered as categorical variables via dummy coding) to ACL stress variance, with both main-effects and interaction models reported (R^2, adjusted R^2, AIC).

Pearson product-moment correlation was used to assess linear relationships among continuous variables; Spearman rank correlation was used as a robustness check. The significance threshold was

set at $P < 0.05$ (two-tailed). All statistical analyses were performed using Python 3.10 with SciPy 1.11 and statsmodels 0.14.

To account for the repeated-measures structure of the data (six flexion angles per graft diameter), a linear mixed-effects model (LMM) was additionally fitted with graft diameter as a fixed effect and flexion angle as a random intercept. The intraclass correlation coefficient (ICC) was reported to quantify the proportion of variance explained by the angle grouping. Post-hoc power analysis was conducted using G*Power methodology based on the observed effect size.

Model Validation and Mesh Quality

The native knee mesh comprised approximately 270,000–400,000 elements, and each of the three reconstruction models comprised approximately 610,000–670,000 elements across six flexion angles, with refined element sizes in ligament insertion sites and cartilage layers. Mesh density was selected based on standard finite element practice for knee joint modeling, balancing computational accuracy and efficiency.

Model validation was conducted through quantitative comparison with published experimental and computational data. Under 134 N anterior loading at 30° flexion (kinematically equivalent to the 134 N posterior force applied to the femur in our model), the native ACL force predicted by our model was within the range reported by previous experimental and computational studies (100–180 N) [6,10]. The tibiofemoral contact pressure distribution and peak contact pressure (approximately 3.5–4.5 MPa) were consistent with values reported in the literature for intact knees [8,17]. Additionally, the anterior tibial translation under 134 N load (approximately 0.4–5.6 mm) fell within the experimentally measured range [12,18]. These comparisons confirmed that the model reproduced physiological knee biomechanics within acceptable limits.

Key model parameters are summarized as follows: the model included femur, tibia, fibula, patella, medial and lateral menisci, articular cartilage, the ACL, posterior cruciate ligament (PCL), medial collateral ligament (MCL), and lateral collateral ligament (LCL). Patella and femur were assigned an elastic modulus of 1200 MPa (Poisson's ratio 0.38), tibia and fibula 6900 MPa (Poisson's ratio 0.49), the ACL graft (hamstring tendon) 116 MPa (Poisson's ratio 0.30), the native ACL 116 MPa (Poisson's ratio 0.30), the PCL 87 MPa (Poisson's ratio 0.30), collateral ligaments 48 MPa (Poisson's ratio 0.30), medial and lateral menisci 5 MPa (Poisson's ratio 0.46), and articular cartilage 5 MPa (Poisson's ratio 0.46), consistent with established knee finite element models [2,8,16,17]. All contacts were defined as frictionless surface-to-surface interactions. The tibia and fibula were fully constrained at their inferior surfaces, while the loading was applied to the femur.

Sensitivity Analyses

Four sensitivity analyses were performed to assess the robustness of the primary findings. First, bootstrap resampling (10,000 iterations) was used to estimate 95% confidence intervals (CIs) for pairwise mean differences in peak graft stress between diameters. Second, leave-one-factor-out analyses sequentially excluded each flexion angle (six scenarios) and each loading condition (five scenarios), with the diameter ranking of mean peak stress re-estimated in each scenario. Third, the diameter × flexion angle interaction was re-tested after exclusion of each single angle to determine whether the interaction was driven by any specific position. Fourth, the primary diameter effect was re-examined using the Kruskal–Wallis test as a distribution-free confirmation. All sensitivity analyses

were performed on the complete set of 90 reconstructed-knee simulations using the same statistical environment as the primary analysis. Because the anatomical basis of the model is a single volunteer, this study is positioned as an in-silico exploratory analysis: the sensitivity analyses above were designed to establish the stability of the diameter ranking and of the diameter x flexion angle interaction across analytical scenarios, rather than of the absolute stress magnitudes, thereby providing a structured methodological compensation for the single-specimen design.

Results

Overall ACL Stress by Graft Diameter

Across all 90 reconstructed analyses, ACL peak stress increased with graft diameter: 12.16 ± 4.94 MPa (7 mm), 14.31 ± 6.24 MPa (8 mm), and 17.00 ± 8.07 MPa (9 mm). One-way ANOVA revealed a significant overall difference among diameters ($F = 4.125$, $P = 0.020$, $\eta^2 = 0.087$, medium effect). Post-hoc Bonferroni-corrected comparisons showed that the 9 mm graft had significantly higher stress than the 7 mm graft (mean difference = 4.84 MPa, raw $P = 0.007$, Bonferroni-adjusted $P = 0.021$, Cohen's $d = 0.74$, medium effect); differences between 8 mm and 7 mm ($P = 0.431$) and between 9 mm and 8 mm ($P = 0.463$) did not reach significance (Figure 2A; Table 2).

Two-way ANOVA (diameter × angle) demonstrated significant main effects for both diameter ($F = 17.92$, $P < 0.001$, ordinary $\eta^2 = 0.087$, i.e., 8.7% of total variance) and flexion angle ($F = 55.73$, $P < 0.001$, $\eta^2 = 0.673$, large effect), as well as a significant diameter-angle interaction ($F = 2.74$, $P = 0.006$, $\eta^2 = 0.066$, medium effect). Multiple linear regression showed that the main-effects model (diameter + angle + condition) explained 81.8% of stress variance (adjusted $R^2 = 0.792$, AIC = 469.5); adding the diameter-angle interaction increased R^2 to 88.4% (adjusted $R^2 = 0.848$, AIC = 449.0). As continuous predictors, each 1 mm increase in graft diameter was associated with a 2.42 MPa increase in ACL stress ($P < 0.001$), and each 10-degree increase in flexion angle was associated with a 1.81 MPa increase ($P < 0.001$) (Figure 2B).

Pearson correlation analysis confirmed that flexion angle was the strongest correlate of ACL stress ($r = 0.796$, $P < 0.001$; note that the stress–angle relationship is non-monotonic, with relative troughs at 15° and 45°, so this coefficient should be interpreted as association strength rather than a linear trend), while graft diameter showed a weaker but significant positive correlation ($r = 0.294$, $P = 0.005$). ACL and PCL stress were significantly positively correlated ($r = 0.738$, $P < 0.001$), reflecting cooperative load-sharing within the cruciate ligament system.

Sensitivity analysis was performed by removing the 15° external rotation condition (the most extreme outlier). After this exclusion, the diameter-stress relationship remained significant ($r = 0.292$, $P = 0.006$; one-way ANOVA $F = 3.937$, $P = 0.023$), confirming that the overall findings were not driven solely by the high-stress outlier condition. Stratified analysis by flexion range revealed that the diameter effect was most pronounced at 90° deep flexion ($F = 115.259$, $P < 0.001$), where mean stress was 15.36 ± 1.04 MPa (7 mm), 22.40 ± 1.28 MPa (8 mm), and 29.37 ± 1.92 MPa (9 mm). At moderate flexion (30°–60°), the diameter effect showed a trend toward significance ($F = 2.683$, $P = 0.080$), while at low flexion (0°–15°), no significant diameter effect was detected ($F = 0.554$, $P = 0.581$).

Linear mixed-effects modeling confirmed the robustness of the diameter effect after accounting for the repeated-measures structure. Graft diameter remained a significant predictor of ACL stress ($\beta = 2.42$ MPa/mm, $z = 5.426$, $P < 0.001$), with flexion angle as a random intercept explaining 75.1% of the total variance (ICC = 0.751). The diameter-angle interaction was also significant in the mixed model ($\beta = 0.063$, $z = 4.655$, $P < 0.001$), confirming that the effect of diameter increases with flexion angle. Post-hoc power analysis indicated 72.9% power for the observed effect size (Cohen's $f = 0.307$), and 92.6% power for detecting large effects (Cohen's $f = 0.40$).

Table 2. ACL peak stress statistics by graft diameter (90 analyses)

Diameter	Mean (MPa)	SD	Median (MPa)	95% CI	Min (MPa)	Max (MPa)
7 mm	12.16	4.94	14.08	[10.32, 14.00]	2.65	18.89
8 mm	14.31	6.24	15.67	[11.98, 16.64]	3.09	23.90
9 mm	17.00	8.07	16.78	[13.99, 20.02]	3.80	31.61

To provide clinical context, estimated graft force was calculated as the product of peak stress and graft cross-sectional area (7 mm: 38.48 mm²; 8 mm: 50.27 mm²; 9 mm: 63.62 mm²). This estimation assumes uniform stress distribution and therefore represents an upper-bound estimate; actual graft force is likely lower due to non-uniform stress distribution. Across all analyses, estimated mean graft force was 468 N (7 mm), 719 N (8 mm), and 1082 N (9 mm). At 90° deep flexion, estimated force reached 591 N (7 mm), 1126 N (8 mm), and 1868 N (9 mm). These estimates are comparable to physiological ACL force levels reported for daily activities (approximately 100–300 N during walking and 500–1,000 N during running) [3,12]; however, the 9 mm graft exceeds the upper bound even on average (1,082 N), and at 90° deep flexion the 8 mm (1,126 N) and 9 mm (1,868 N) grafts markedly exceed it, suggesting potential overload in deep squatting positions (Table 3).

Table 3. Estimated ACL graft force based on peak stress and cross-sectional area

Diameter	Cross-section (mm²)	Relative stiffness	Mean stress (MPa)	Est. mean force (N)	90° stress (MPa)	Est. 90° force (N)
7 mm	38.48	1.00×	12.16	468	15.36	591
8 mm	50.27	1.31×	14.31	719	22.40	1126
9 mm	63.62	1.65×	17.00	1082	29.37	1868

Finally, an exploratory fatigue life estimation was performed by applying an experimentally derived tendon fatigue S-N curve ($S = 101.3 - 14.8 \times \log(N)$), established from cyclic loading tests of human extensor tendons [29,30], to the quasi-static peak stress values obtained in this study. Because this approach assumes constant-amplitude cyclic loading and a uniform stress distribution, the resulting values are theoretical estimates rather than validated predictions and are reported here for hypothesis generation only. With that caveat, the estimated mean fatigue life was approximately 1.06 million cycles (7 mm), 0.75 million cycles (8 mm), and 0.50 million cycles (9 mm), decreasing at 90° deep flexion to approximately 0.64, 0.21, and 0.07 million cycles, respectively; the 9 mm estimate corresponded to 47% of the 7 mm value under average loading and 11% at 90° deep flexion.

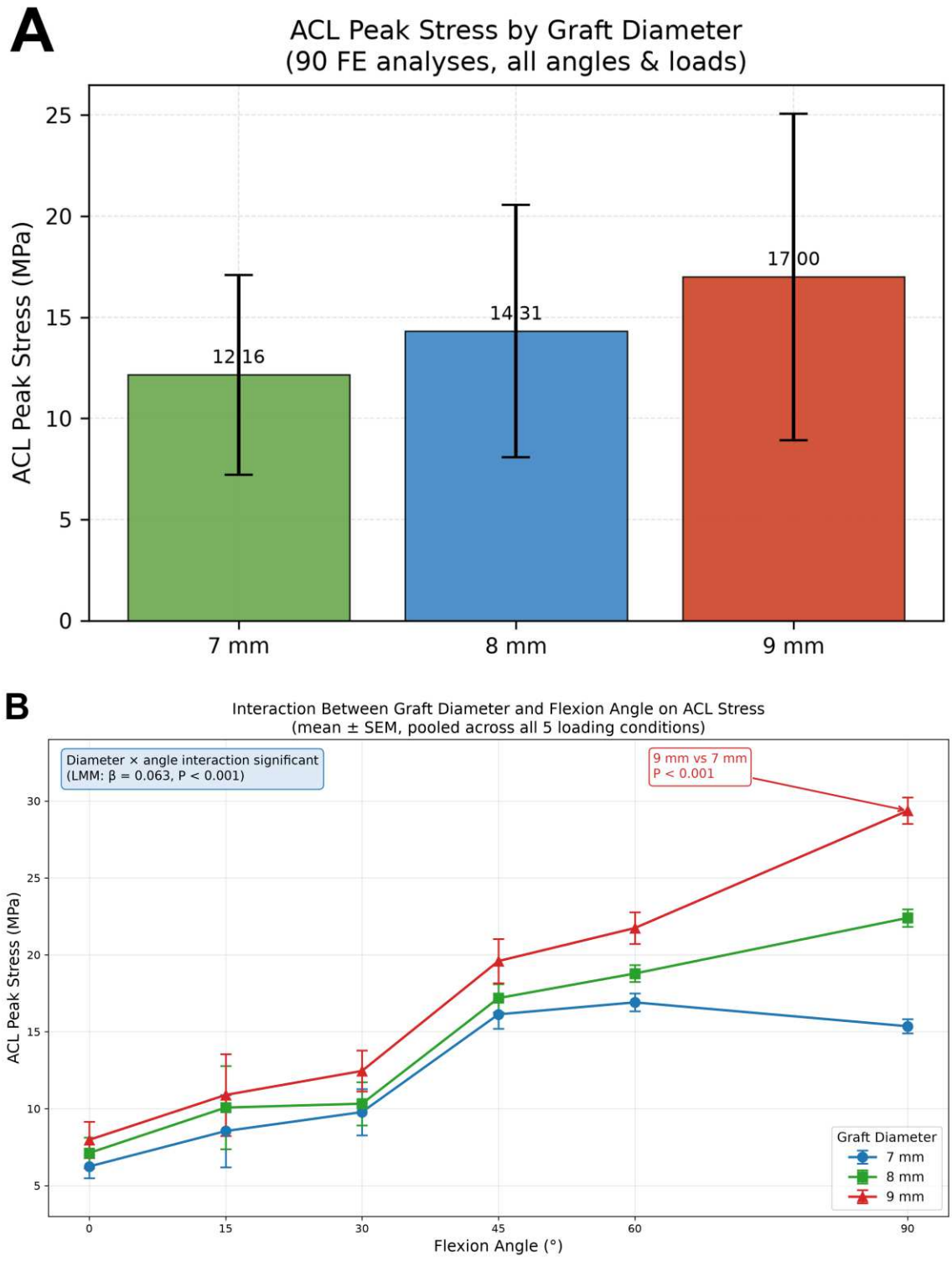


Figure 2. ACL peak stress by graft diameter. (A) Mean peak stress across all 90 analyses (mean ± SD). (B) Diameter–angle interaction effect on ACL stress (mean ± standard error of the mean); the diameter effect became more pronounced at deeper flexion angles (LMM: $\beta = 0.063$, $P < 0.001$).

Low Flexion (0°–15°): External Rotation as High-Risk Position

At 0° extension, ACL stress was relatively low for all graft sizes (3.78–11.05 MPa). At 15° flexion under external rotation, a pronounced diameter-dependent stress elevation was observed: native ACL bore minimal stress (1.95 MPa), while reconstructed grafts reached 14.43–18.07 MPa, representing 7.4–9.3 times the native level. Because the native ACL bears a minimal stress denominator at this position (1.95 MPa, only 6.5% of its 30° external-rotation value), this relative ratio is amplified by the low denominator, with an absolute increment of only 12–16 MPa; nevertheless, reconstructed grafts do bear marked tension during slight flexion with external rotation, a motion commonly encountered in early rehabilitation (Figure 3).

At 15° internal rotation, ACL stress was substantially lower (2.65–3.80 MPa) and remained below native levels (4.74 MPa), ranging from 0.56 to 0.80 times the native value. Internal rotation at 15° flexion thus produced the lowest graft stress values observed in this study.

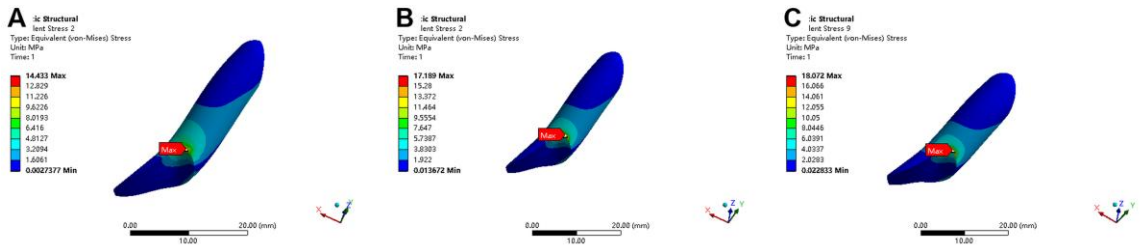


Figure 3. ACL graft stress contours at 15° flexion under 8 N·m external rotation. (A) 7 mm graft (peak stress: 14.43 MPa). (B) 8 mm graft (peak stress: 17.19 MPa). (C) 9 mm graft (peak stress: 18.07 MPa). Note the progressive increase in peak stress and stress concentration area with larger graft diameter, with marked stress concentration in the ligament mid-substance and at the bone tunnel exit.

Moderate Flexion (30°–60°): Reconstructed ACL Below Native Level

At 30° and 60°, native ACL undertook high physiological load (29.16–30.15 MPa under external rotation). Reconstructed graft stress was substantially lower than native levels at 30° (15.28–16.30 MPa, only 51%–54% of native) and moderately lower at 60° (17.36–19.75 MPa, 60%–68% of native). Reconstructed graft stress thus remained consistently below physiological levels throughout the mid-flexion range (Figure 4; Table 4).

Table 4. ACL peak stress at each flexion angle under 8 N·m external rotation

Angle	Native (MPa)	7 mm	8 mm	9 mm	9mm/Native
0°	6.48	7.15	8.96	10.32	1.59×
15°	1.95	14.43	17.19	18.07	9.27×
30°	30.15	15.28	15.35	16.30	0.54×
45°	10.67	14.13	15.99	15.52	1.45×

60°	29.16	17.36	18.98	19.75	0.68×
90°	21.38	15.96	23.06	30.47	1.43×

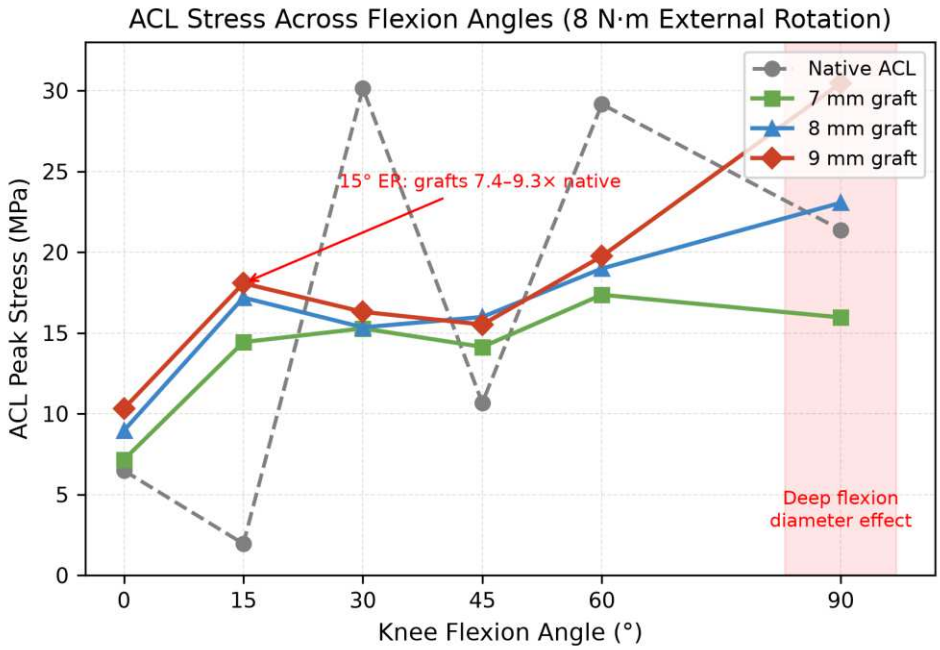


Figure 4. ACL stress across flexion angles under 8 N·m external rotation, with native knee control.

Deep Flexion (90°): Most Pronounced Diameter Effect

At 90° deep flexion, the diameter effect was most pronounced. Under external rotation, the 9 mm graft exhibited peak stress of 30.47 MPa, exceeding native ACL (21.38 MPa) by 42.5%. The 7 mm graft showed insufficient load-bearing (15.96 MPa, 74.6% of native). The 8 mm graft achieved near-physiological stress (23.06 MPa, 107.8% of native)—the closest approximation to physiological loading among the three diameters at this functionally demanding position. The stress difference between 9 mm and 7 mm at 90° reached 91%, far exceeding other flexion angles (Figures 5 and 6A).

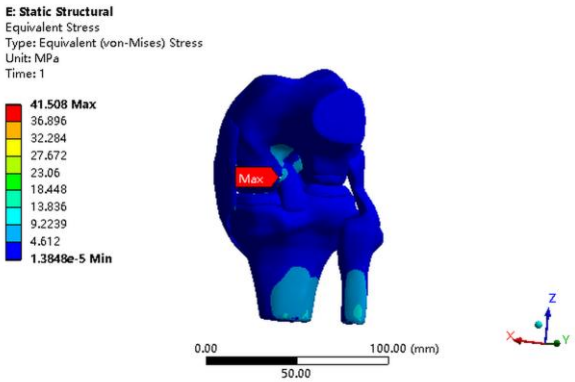


Figure 5. Overall knee stress contour at 90° deep flexion. Stress concentration is observed in the intercondylar notch and graft tunnel outlet.

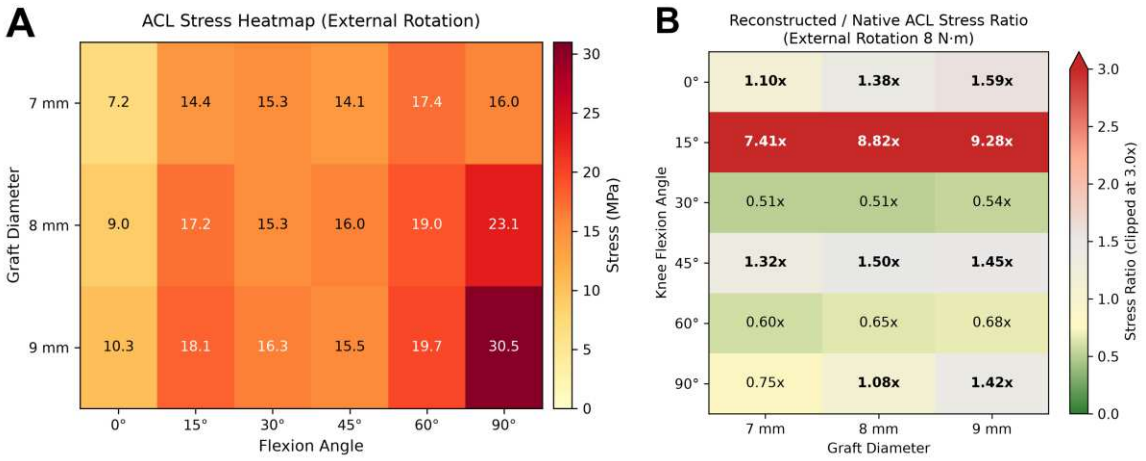


Figure 6. Heatmaps of ACL stress across flexion angle and graft diameter under 8 N·m external rotation. (A) Peak ACL stress; the 90° + 9 mm region shows the highest stress. (B) Reconstructed-to-native ACL stress ratio; red indicates supra-physiological stress.

Loading Condition Effect

ACL stress varied across loading conditions. Internal rotation produced the highest diameter-dependent increase (9/7 ratio = 1.54), followed by posterior load (1.41), valgus (1.40), varus (1.37), and external rotation (1.31). The positive diameter-stress relationship was consistent across all five loading conditions. Although the 9/7 stress ratio was highest under internal rotation, the diameter effect size was greatest under external rotation ($\eta^2 = 0.126$), which also produced the highest absolute stress levels (Figure 7; Table 5).

Table 5. Mean ACL peak stress under five loading conditions

Condition	7 mm	8 mm	9 mm	9/7 Ratio
Internal rotation 8 N·m	10.16	12.06	15.67	1.54
External rotation 8 N·m	14.05	16.59	18.40	1.31
Varus 20 N·m	12.88	15.54	17.60	1.37
Valgus 20 N·m	10.62	11.91	14.88	1.40
Posterior load 134 N	13.07	15.46	18.46	1.41

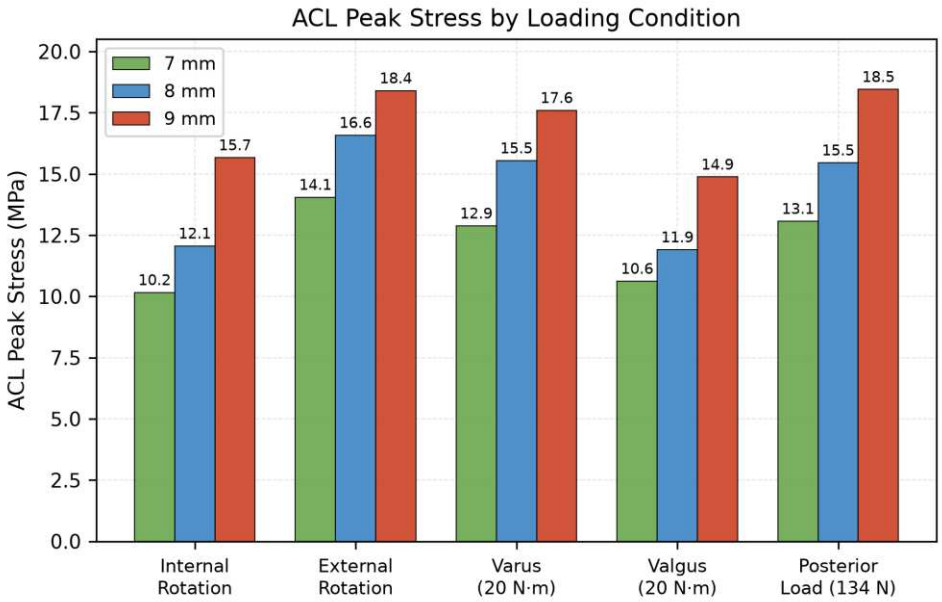


Figure 7. ACL peak stress comparison across five loading conditions.

PCL Stress: Mild Compensatory Increase

After ACL reconstruction, PCL stress increased mildly compared to native knee. Under rotation conditions, mean PCL stress was 31.71 MPa (7 mm), 30.88 MPa (8 mm), and 30.01 MPa (9 mm), compared to 23.06 MPa in the native knee — representing approximately 1.30–1.37 times the native level. Notably, PCL stress decreased as graft diameter increased, suggesting that larger ACL grafts bear more load and reduce PCL compensation (Figure 8A).

ACL–PCL Coupling and Diameter Gradient

ACL and PCL stress showed significant positive correlation ($r = 0.738$, $P < 0.001$), reflecting cooperative load-sharing within the cruciate ligament system. The 7 mm graft showed acceptable low-angle biomechanics but insufficient deep flexion stability. The 8 mm graft achieved the most favorable trade-off between adequate graft loading and avoidance of supra-physiological stress; although the 7 mm graft tracked native stress more closely at low flexion angles, its deep-flexion under-loading raises long-term stability concerns. The 9 mm graft exhibited supra-physiological stress primarily at 90° deep flexion and 15° external rotation (Figure 8B).

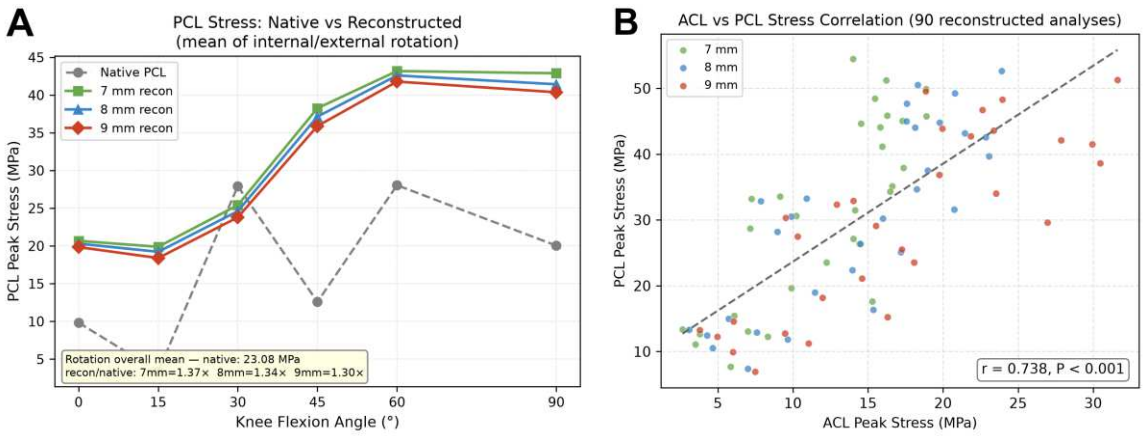


Figure 8. Posterior cruciate ligament (PCL) response. (A) PCL stress comparison between native and reconstructed knees (mean of internal/external rotation); PCL stress increases mildly (approximately 1.30–1.37×) and decreases with larger graft diameter. (B) Correlation scatter plot of ACL and PCL peak stress (r = 0.738, P < 0.001).

Comparison With Native Knee

In 12 matched rotation conditions (6 angles × 2 rotations), 7 mm grafts showed below-native ACL stress in 8 of 12 conditions (67%), while 8 mm and 9 mm grafts each showed below-native stress in 6 of 12 conditions (50%). The 9 mm graft exceeded native stress primarily at 90° deep flexion (all five loading conditions) and at 0°, 15°, and 45° under external rotation. This indicates that while larger grafts increase peak stress, the majority of reconstructed knees operate within or below physiological stress ranges (Figures 6B and 9).

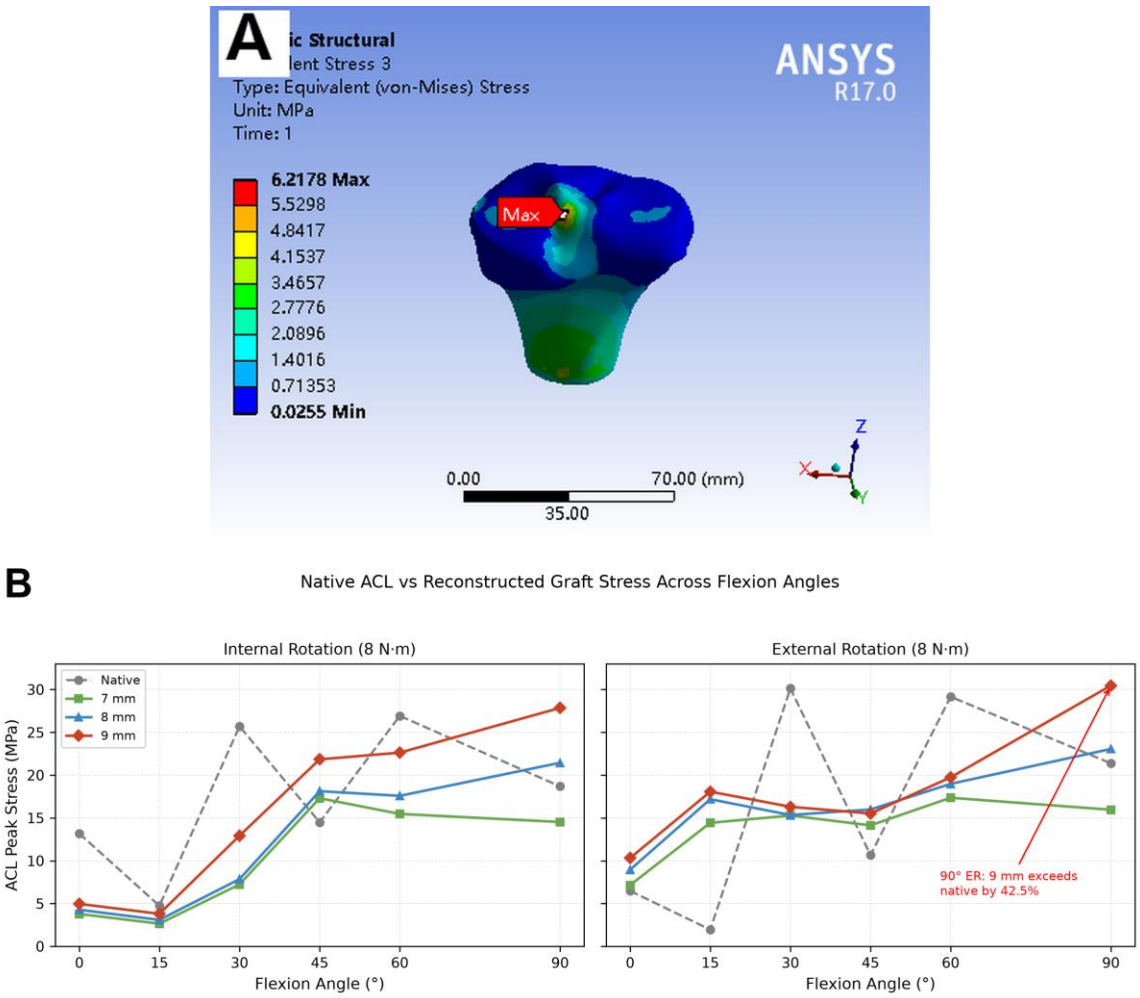


Figure 9. Native knee control. (A) Native knee stress contour (control baseline); stress distribution is uniform under physiological loading. (B) Native ACL versus reconstructed graft stress across flexion angles (internal and external rotation dual panels).

Sensitivity and Robustness Analyses

Bootstrap analysis confirmed that the stress difference between the two extreme diameters was robust (9 mm vs 7 mm: mean difference 4.82 MPa, 95% CI 1.46–8.16), whereas differences between adjacent diameters did not reach statistical significance (8 mm vs 7 mm: 2.15 MPa, 95% CI -0.65 to 5.00; 9 mm vs 8 mm: 2.70 MPa, 95% CI -0.89 to 6.34). This pattern is consistent with clinical and biomechanical evidence indicating that measurable differences arise primarily between extreme graft sizes rather than between adjacent sizes [21,31]. The monotonic diameter ranking (7 < 8 < 9 mm) was

preserved in all eleven leave-one-factor-out scenarios, confirming that the diameter effect was not driven by any single flexion angle or loading condition. The diameter × angle interaction remained significant after exclusion of any single flexion angle (all $P \leq 0.002$) except 90° ($P = 0.97$), indicating that the interaction was specifically driven by deep flexion and reinforcing the conclusion that the diameter effect peaks at 90°. The primary diameter effect was further confirmed by the Kruskal–Wallis test ($H = 6.49$, $P = 0.039$), indicating that the findings do not depend on parametric distributional assumptions.

Discussion

Principal Findings

This study compared three commonly used ACL graft diameters (7, 8, and 9 mm) against a native knee control across 120 finite element simulations. The principal finding is that graft diameter exerts a significant independent effect on peak intra-graft stress ($F = 17.92$, $P < 0.001$, $\eta^2 = 0.087$), with each 1 mm increase associated with a 2.42 MPa stress elevation. On average, the 9 mm graft demonstrated 40% higher peak stress than the 7 mm graft (17.0 vs 12.2 MPa). This observation is consistent with recent clinical evidence suggesting that grafts larger than 8 mm may be associated with increased failure risk [22], although the relationship remains debated in the literature [13]. These principal findings remained stable across bootstrap resampling, leave-one-factor-out scenarios, and distribution-free testing (see Sensitivity and robustness analyses).

Meanwhile, the diameter effect of the reconstructed ACL is position-dependent rather than uniform. In approximately 56% of the matched rotation conditions (20/36 across all three graft diameters), reconstructed ACL stress remained below native levels—predominantly at 30°–60° flexion and under internal rotation—indicating that grafts generally under-load during routine activities. Supra-physiological stress was concentrated in two specific positions: (1) 90° deep flexion, where the 9 mm graft exceeded native stress by 42.5%; and (2) 15° flexion with external rotation, where all graft sizes reached 7.4–9.3 times the native ACL stress. The latter finding requires cautious interpretation: the native ACL bears minimal load at this position (1.95 MPa), so the low denominator amplifies the relative ratio (absolute increment only 12–16 MPa); in contrast, the absolute stress elevation of the 9 mm graft at 90° deep flexion (30.47 MPa, 1.43 times native) is of greater clinical relevance.

Mechanisms Underlying the Diameter-Stress Relationship

Three biomechanical mechanisms account for the observed diameter-stress relationship. First, larger grafts possess greater structural stiffness (EA), where E is elastic modulus and A is cross-sectional area. In a multi-ligament knee system, external load is distributed among restraining structures according to their relative stiffness; a stiffer graft therefore bears a greater share of the applied load [23,24]. Since all graft diameters in this study used identical material properties (E constant), relative stiffness is determined solely by cross-sectional area: 7 mm (38.48 mm², 1.00×), 8 mm (50.27 mm², 1.31×), and 9 mm (63.62 mm², 1.65×). Consistently, a previous finite element study demonstrated that increasing graft Young's modulus directly increases graft force, and that when stiffer materials are used, smaller diameter grafts are required to maintain physiological graft force [23].

Second, larger grafts occupy a greater volume within the intercondylar notch, increasing the likelihood of mechanical contact with the femoral notch wall during flexion. This impingement generates additional contact stress, particularly at low flexion angles where graft orientation deviates most from

the native ACL path [4,25]. Clinically, graft-notch impingement is associated with cyclops lesion formation and loss of extension [25]. Both mechanisms are position-dependent, which explains why the diameter effect is not uniformly observed across all flexion angles and loading conditions.

The load-sharing framework also explains the observed mild PCL stress elevation after reconstruction (approximately 1.30–1.37× native). When the reconstructed ACL becomes stiffer than the native ligament, it bears a greater proportion of anterior restraint, potentially reducing PCL loading in anterior drawer. However, the altered kinematics and graft pretension may increase PCL loading in combined rotation and flexion positions, resulting in the observed mild net elevation. This interpretation is consistent with the significant positive correlation between ACL and PCL stress ($r = 0.738$, $P < 0.001$), reflecting cooperative rather than competitive load-sharing within the cruciate ligament system.

Third, fatigue failure theory provides additional mechanistic insight into the diameter-stress relationship. Ligament and tendon tissues exhibit classic fatigue behavior: maximal cyclic loading leads to progressive collagen fiber damage, cumulative microtears, and eventual catastrophic failure. Experimental studies of human tendon demonstrate a log-linear S-N relationship ($S = 101.3 - 14.8 \times \log(N)$) with no true endurance limit, meaning that even physiological stress levels will eventually cause failure given sufficient cycles [29,30]. In this study, the estimated theoretical fatigue life of the 9 mm graft was 47% of the 7 mm graft under average loading conditions and only 11% at 90° deep flexion. At 90° deep flexion, the 9 mm graft had an estimated fatigue life of only 72,000 cycles, which could be accumulated within months of daily activities involving deep knee bending. This suggests that larger-diameter grafts, while possessing greater ultimate strength, may experience accelerated fatigue accumulation due to their higher operating stress, particularly in repetitive deep flexion activities such as squatting and stair climbing. Clinically, this may manifest as late graft failure or gradual graft laxity years after reconstruction, consistent with clinical reports of increased revision rates associated with larger grafts in some cohorts [22]. These fatigue estimates are exploratory and hypothesis-generating; they should not be interpreted as quantitative predictions of in-vivo graft survival.

The fatigue mechanism also explains the position-dependence of the diameter effect. At low flexion angles (0°–15°), ACL stress is relatively low for all graft sizes, and the estimated fatigue life exceeds 500,000 cycles. At 90° deep flexion, however, the stress elevation in larger grafts becomes critical, reducing the 9 mm graft fatigue life to only 72,000 cycles. This position-dependent fatigue risk has direct implications for rehabilitation: activities involving repetitive deep flexion should be restricted in the early postoperative period, particularly for patients with larger-diameter grafts. As noted above, these figures are theoretical extrapolations derived from quasi-static stress values and should be interpreted with caution.

Clinical Implications

The 8 mm graft represented the most favorable trade-off across the evaluated criteria. At 90° deep flexion, its stress under external rotation reached 107.8% of native ACL (23.06 vs 21.38 MPa)—the closest approximation to physiological loading among the three diameters at this functionally demanding position. Although the 7 mm graft tracked native values more closely at low flexion angles (0°–45°), its mean deviation from native stress under external rotation was only marginally smaller than that of the 8 mm graft (8.12 vs 8.28 MPa), while its deep-flexion under-loading raises distinct long-term stability concerns (see ACL-PCL coupling and diameter gradient). A recent meta-analysis of 46,268 patients found that hamstring autografts smaller than 8 mm had 46% greater odds of graft

failure compared with grafts of 8 mm or larger [21], supporting the clinical relevance of an 8 mm threshold.

The 7 mm graft may be appropriate for patients with small body habitus, but its stress at deep flexion reached only 65%–77% of native levels (74.6% under external rotation at 90°), suggesting insufficient load transfer that may contribute to long-term graft laxity. The 9 mm graft is not recommended for routine use due to consistent supra-physiological stress at 90° flexion and 15° external rotation [22].

For postoperative rehabilitation, the combination of 15° flexion and external rotation should be avoided in the early phase, as this position generates 7.4–9.3 times the native ACL stress. Graft pretension is another important variable: excessive initial tension can over-constrain the knee and increase graft force, while insufficient tension compromises stability [26,27]. PCL stress increased mildly after reconstruction (approximately 30%–37%), consistent with a prior finite element study reporting altered PCL loading after ACL reconstruction [28].

Clinical and Biomechanical Findings

Previous clinical cohort studies have demonstrated a clear dose-response gradient: smaller grafts (< 8 mm) carry significantly higher failure risk, while the protective effect plateaus at ≥9 mm, with no additional benefit beyond 10 mm [9,11,15]. This has led to the widespread clinical practice of maximizing graft diameter. In contrast, the present finite element analysis demonstrates that larger graft diameter is associated with progressively higher peak intra-graft stress (7 mm: 12.16 MPa; 8 mm: 14.31 MPa; 9 mm: 17.00 MPa), with the 9 mm graft exhibiting supra-physiological stress at 90° flexion and 15° external rotation. However, it must be made clear that peak stress is not equivalent to failure risk. Clinical graft failure is a multifactorial outcome influenced by biological integration, tunnel enlargement, immune response, and rehabilitation adherence, in addition to mechanical stress [13,20]. A graft with higher peak stress may still possess greater overall load-bearing capacity due to its larger cross-sectional area. Indeed, biomechanical testing of hamstring grafts demonstrated mean failure loads of 3,263 ± 677 N (7 mm), 3,908 ± 556 N (8 mm), and 4,360 ± 606 N (9 mm); although strength increased significantly across the full range, differences between adjacent diameters within 7–9 mm did not reach significance, and the incremental strength gain diminished from 38% (6 to 7 mm) to 12% (8 to 9 mm), suggesting that the structural benefit of larger grafts plateaus within this diameter range [31].

Second, the clinical plateau effect at ≥9 mm may itself reflect the balance between increasing structural stiffness and increasing peak stress. Below 8 mm, the primary failure mode is insufficient structural strength (graft rupture or elongation). At 8–9 mm, structural strength is adequate, but peak stress begins to rise, potentially contributing to fatigue failure and tunnel widening. Beyond 9–10 mm, the additional structural benefit is offset by increased notch impingement risk and higher peak stress. A 2024 cohort study of 1,730 patients found that grafts >8 mm were associated with a 1.64–2.19 times higher risk of overall graft failure, although the adjusted analysis did not reach statistical significance [22]. Notably, the diameter range examined in this study (7–9 mm) corresponds to the clinically critical threshold zone. The clinical dose-response gradient is most pronounced below 8 mm, while the plateau and potential risk increase occur at ≥9 mm. The 8 mm graft emerges as the most favorable balance point: it avoids the high failure risk associated with <8 mm grafts while minimizing the peak stress elevation and notch impingement risk associated with ≥9 mm grafts. This biomechanical interpretation aligns with the clinical observation that 8 mm is the most commonly achieved and recommended graft diameter in contemporary practice [21].

Limitations

Several limitations should be acknowledged. First, all stress measurements represent peak von Mises stress (maximum element value), not average stress over the ligament substance. At geometric discontinuities such as tunnel outlets and ligament insertion sites, peak stress is susceptible to stress singularity, where values increase with mesh refinement and may not converge to a finite limit [6,16,26]; therefore, absolute peak stress magnitudes should be interpreted with caution, while relative differences between graft diameters are more reliable than absolute values.

Second, ligaments were modeled as homogeneous, isotropic, linearly elastic materials, which does not capture the viscoelastic and anisotropic properties of native ligament tissue [6,18]. The use of linear elastic materials may overestimate stress at high strain levels. Third, a single knee geometry was used, limiting generalizability to anatomical variations such as intercondylar notch width and ACL footprint area. Although this precludes population-level inference, the leave-one-factor-out and bootstrap analyses described above demonstrated that the diameter ranking of mean peak stress remained unchanged across all 11 resampling scenarios, indicating that the principal conclusions are not driven by any single flexion angle or loading condition within this geometry. Fourth, cyclic loading, graft creep, and biological remodeling over time were not simulated. Fifth, the high stress observed at 15° external rotation may be influenced by graft pretension, which is known to significantly affect knee kinematics and graft force [27]. Sixth, model validation was performed through literature comparison — ACL force, tibiofemoral contact pressure, and load-induced displacement all fell within ranges reported by published cadaveric and computational studies (see Model validation and mesh quality) — rather than direct experimental validation on the same specimen. Seventh, the tendon–bone healing interface and its biological integration over time were not modeled; actual graft forces during the early postoperative healing phase may differ from the steady-state predictions of this model. Eighth, the applied 8 N·m/20 N·m torques and 134 N anterior drawer force represent clinical-examination/extreme load levels; the resulting stresses and graft forces therefore depict upper-bound scenarios and should not be extrapolated directly to graft forces during routine daily activities. Ninth, formal mesh convergence testing and material-property sensitivity analyses were not performed, because the original solver files were not retained after completion of the simulation campaign. This limitation is partially mitigated by three considerations: the adopted mesh density (approximately 610,000–670,000 elements, with regional refinement at ligament insertions and cartilage layers) is comparable to that of published knee finite element studies [8,17,26]; every conclusion in this study rests on relative differences between graft diameters computed under an identical mesh and an identical set of material properties, rather than on absolute stress magnitudes; and the four sensitivity analyses described above provide an indirect check on the stability of those relative differences across resampling scenarios. The absolute peak stress values nevertheless remain subject to the mesh dependence described in the first limitation. Tenth, the fatigue life estimates are exploratory extrapolations: they were obtained by applying a published S-N curve derived from human extensor tendon under constant-amplitude cyclic loading [29,30] to quasi-static peak stress values from a single specimen, and they do not account for variable-amplitude loading, stress redistribution during tendon-bone healing, or biological remodeling. Future studies incorporating average stress analysis, tendon–bone interface modeling, multi-subject models, and prospective clinical validation are warranted.

Conclusions

In this finite element analysis, larger ACL graft diameter was associated with higher peak intra-graft stress, predominantly at 90° deep flexion and 15° external rotation. Reconstructed ACLs operated

below native stress levels in 56% of matched rotation conditions—mainly at 30°–60° flexion—but exceeded them at 0°–15° under external rotation. The 8 mm graft provided the most favorable loading trade-off and is supported by recent clinical evidence as a favorable threshold. Clinically, these findings identify 90° deep flexion and 15° flexion with external rotation as high-risk positions that warrant protection during early postoperative rehabilitation. These findings are based on peak stress measurements and should be further validated through average stress analysis and prospective clinical studies.

List of abbreviations

ACL: anterior cruciate ligament; PCL: posterior cruciate ligament; MCL: medial collateral ligament; LCL: lateral collateral ligament; LMM: linear mixed-effects model; ICC: intraclass correlation coefficient; ANOVA: analysis of variance; CI: confidence interval; SD: standard deviation; SEM: standard error of the mean; AIC: Akaike information criterion; FEA: finite element analysis; EA: structural stiffness (elastic modulus x cross-sectional area); MPa: megapascal; N-m: newton-metre

Declarations

Ethics approval and consent to participate: This study was approved by the Ethics Committee of the First Affiliated Hospital of Guangdong Pharmaceutical University, Guangzhou, Guangdong, China, as a sub-study of the post-market clinical evaluation programme "A prospective, single-center, single-arm, performance-goal-based study to evaluate the safety and effectiveness of Mindray knee joint products for total knee arthroplasty" (approval number: IIT No. (60); date of approval: 22 September 2025). The study was conducted in accordance with the Declaration of Helsinki. All imaging data were obtained from a healthy adult volunteer who provided written informed consent for the use of the anonymized images for research purposes, and no personally identifiable information is presented in this article.

Consent for publication: Not applicable.

Availability of data and materials: The datasets generated and analysed during the current study, together with the custom Python code used for the statistical analysis, are available from the corresponding authors on reasonable request.

Competing interests: The authors declare that they have no competing interests.

Funding: This work was supported by the Guangzhou Science and Technology Plan Project (Grant No. 2025A03J3719), the Open Project Program of the State Key Laboratory of Neurology and Oncology Drug Development (Grant No. SKLSIM-F-2025009), the "Discipline Cultivation and Innovation Enhancement" Special Major Project of Guangdong Pharmaceutical University (Grant No. XKPYZD20260811), and the post-market clinical evaluation programme "A prospective, single-center, single-arm, performance-goal-based study to evaluate the safety and effectiveness of Mindray knee joint products for total knee arthroplasty". The funders had no role in the study design, data collection and analysis, decision to publish, or preparation of the manuscript.

Authors' contributions: Shaolong Du conceived the study, performed the finite element analysis, conducted the statistical analysis, and drafted the manuscript. Xishan Li participated in data analysis,

literature review, and manuscript revision. Qiang Lin contributed to study design, data curation, and manuscript revision. Xuehui Luo supervised the study, provided clinical expertise, and revised the manuscript critically. All authors read and approved the final manuscript.

Acknowledgements: The authors thank the healthy volunteer who provided the imaging data used for finite element model construction.

Use of artificial intelligence: During the preparation of this work, the authors used AI-assisted tools (large language models) for language polishing and manuscript formatting. All content was reviewed, verified, and edited by the authors, who take full responsibility for the integrity and accuracy of the published work.

References

[1] Mehl J, Otto A, Baldino JB, et al. The ACL-deficient knee and the prevalence of meniscus and cartilage lesions: a systematic review and meta-analysis. Arch Orthop Trauma Surg. 2019;139(6):819-841.

[2] Bendjaballah MZ, Shirazi-Adl A, Zukor DJ. Biomechanics of the human knee joint in compression: reconstruction, mesh generation and finite element analysis. Knee. 1995;2(2):69-79.

[3] Besier TF, Fredericson M, Gold GE, Beaupre GS, Delp SL. Knee muscle forces during walking and running in patellofemoral pain patients and pain-free controls. J Biomech. 2009;42(7):898-905.

[4] Duthon VB, Barea C, Abrassart S, et al. Anatomy of the anterior cruciate ligament. Knee Surg Sports Traumatol Arthrosc. 2006;14(3):204-213.

[5] Orozco GA, Stenroth L, Esrafilian A, et al. Effect of patient specificity on predicting knee cartilage degeneration in obese adults: musculoskeletal finite-element modeling of data from the CAROT trial. J Orthop Res. 2024;42(11):2437-2449.

[6] Weiss JA, Gardiner JC. Computational modeling of ligament mechanics. Crit Rev Biomed Eng. 2001;29(3):303-371.

[7] Gianotti SM, Marshall SW, Hume PA, Bunt L. Incidence of anterior cruciate ligament injury and other knee ligament injuries: a national population-based study. J Sci Med Sport. 2009;12(6):622-627.

[8] Blankevoort L, Kuiper JH, Huiskes R, Grootenboer HJ. Articular contact in a three-dimensional model of the knee. J Biomech. 1991;24(11):1019-1031.

[9] Mariscalco MW, Flanigan DC, Mitchell J, et al. The influence of hamstring autograft size on patient-reported outcomes and risk of revision after anterior cruciate ligament reconstruction: a multicenter orthopaedic outcomes network (MOON) cohort study. Arthroscopy. 2013;29(12):1948-1953.

[10] Li G, Gil J, Kanamori A, Woo SL. A validated three-dimensional computational model of a human knee joint. J Biomech Eng. 1999;121(6):657-662.

[11] Magnussen RA, Lawrence JTR, West RL, et al. Graft size and patient age are predictors of early revision after anterior cruciate ligament reconstruction with hamstring autograft. Arthroscopy. 2012;28(4):526-531.

[12] Markolf KL, Burchfield DM, Shapiro MM, et al. Combined knee loading states that generate high anterior cruciate ligament forces. J Orthop Res. 1995;13(6):930-935.

[13] Macaulay AA, Perfetti DC, Levine WN. Anterior cruciate ligament graft choices. Sports Health. 2012;4(1):63-68.

[14] Pena E, Calvo B, Martinez MA, Palanca D, Doblaré M. Finite element analysis of the effect of meniscal tears and meniscectomies on human knee biomechanics. Clin Biomech. 2005;20(5):498-507.

[15] Park SY, Oh H, Park S, et al. Factors predicting hamstring tendon autograft diameters and resulting failure rates after anterior cruciate ligament reconstruction. Knee Surg Sports Traumatol Arthrosc. 2013;21(5):1111-1118.

[16] Peters AE, Akhtar R, Comerford EJ, Bates KT. Tissue material properties and computational modelling of the human tibiofemoral joint: a critical review. PeerJ. 2018;6:e4298.

[17] Donahue TLH, Hull ML, Rashid MM, Jacobs CR. A finite element model of the human knee joint for the study of tibio-femoral contact. J Biomech Eng. 2002;124(3):273-280.

[18] Woo SLY, Hollis JM, Adams DJ, Lyon RM, Takai S. Tensile properties of the human femur-anterior cruciate ligament-tibia complex: the effects of specimen age and orientation. Am J Sports Med. 1991;19(3):217-225.

[19] Sanders TL, Maradit Kremers H, Bryan AJ, et al. Incidence of anterior cruciate ligament tears and reconstruction: a 21-year population-based study. Am J Sports Med. 2016;44(6):1502-1507.

[20] Samuelsen BT, Webster KE, Johnson NR, Hewett TE, Krych AJ. Hamstring autograft versus patellar tendon autograft for ACL reconstruction: is there a difference in graft failure rate? A meta-analysis of 47,613 patients. Clin Orthop Relat Res. 2017;475(10):2459-2468.

[21] Hamrin Senorski R, Högberg J, Teow K, et al. Smaller hamstrings autograft size after primary ACL reconstruction is associated with higher odds for graft failure: a meta-analysis on autografts sizes covering 46,268 patients. Knee Surg Sports Traumatol Arthrosc. 2026;34(9):3212-3232. doi:10.1002/ksa.70069

[22] Abudaqqa RY, Elsheoibi AM, Al Mas AJ, et al. The correlation between graft size and graft failure in hamstring autograft anterior cruciate ligament reconstruction. Cureus. 2024;16(2):e55069. doi:10.7759/cureus.55069

[23] Wang H, Fang C, Tao M, et al. Hourglass-shaped grafts are superior to conventional grafts for restoring knee stability and graft force at knee flexion angle of 30° following ACL reconstruction: a finite element analysis. Front Bioeng Biotechnol. 2022;10:967411.

[24] Wang H, Tao M, Shi Q, et al. Graft diameter should reflect the size of the native anterior cruciate ligament (ACL) to improve the outcome of ACL reconstruction: a finite element analysis. Bioengineering (Basel). 2022;9(10):507.

[25] Kambhampati SBS, Gollamudi S, Shanmugasundaram S, et al. Cyclops lesions of the knee: a narrative review of the literature. Orthop J Sports Med. 2020;8(8). doi:10.1177/2325967120945671

[26] Benos L, Stanev D, Spyrou L, et al. A review on finite element modeling and simulation of the anterior cruciate ligament reconstruction. Front Bioeng Biotechnol. 2020;8:967.

[27] Dargel J, Gotter M, Mader K, et al. Biomechanics of the anterior cruciate ligament and implications for surgical reconstruction. Strategies Trauma Limb Reconstr. 2007;2(1):1-12.

[28] Mao ZM, Wang ZW, Xu C, et al. Intra-articular biomechanical changes of the meniscus and ligaments during stance phase of gait circle after different anterior cruciate ligament reconstruction surgical procedures: a finite element analysis. Orthop Surg. 2022;14(12):3367-3377. doi:10.1111/os.13516

[29] Schechtman H, Bader DL. In vitro fatigue of human tendons. J Biomech. 1997;30(8):829-835. doi:10.1016/S0021-9290(97)00033-X

[30] Hubbard RP, Chun KJ. Mechanical responses of tendons to repeated extensions and wait periods. J Biomech Eng. 1988;110(1):11-19. doi:10.1115/1.3108399

[31] Boniello MR, Schwingler PM, Bonner JM, Robinson SP, Cotter A, Bonner KF. Impact of hamstring graft diameter on tendon strength: a biomechanical study. Arthroscopy. 2015;31(6):1084-1090. doi:10.1016/j.arthro.2014.12.023

Supplementary Files

This is a list of supplementary files associated with this preprint. Click to download.

- 04FigureLegends.docx
- Figures.rar